Eur J Nucl Med Mol Imaging (2009) 36:373–381
DOI 10.1007/s00259-008-0961-4

ORIGINAL ARTICLE

Combined evaluation of preoperative FDG uptake on PET, ground-glass opacity area on CT, and serum CEA level: identification of both low and high risk of recurrence in patients with resected T1 lung adenocarcinoma

Kotaro Higashi · Tsutomu Sakuma · Kengo Ito · Seiji Niho · Yoshimichi Ueda · Takeshi Kobayashi · Ryuzo Sekiguchi · Tomoko Takahashi · Takashi Kato · Hisao Tonami

Received: 1 June 2008 / Accepted: 3 September 2008 / Published online: 18 October 2008

Abstract
Purpose Patients with the same pathological stage of lung adenocarcinoma display marked variability in postoperative recurrence. The aim of this study was to predict the postoperative prognosis in patients with small-sized pulmonary adenocarcinoma on the basis of FDG uptake on PET, the extent of ground-glass opacity (GGO) on CT, and serum carcinoembryonic antigen (CEA) levels.
Methods We evaluated 87 patients (40 men, 47 women; mean age 64 years, age range 42–84 years) with lung adenocarcinoma of 3.0 cm or smaller. The level of FDG uptake (low or high), the extent of GGO (GGO or solid), and serum CEA levels (<20 ng/ml or ≥20 ng/ml) were correlated with the pathological findings of cell dedifferentiation, aggressiveness, N factor, and the incidence of relapse.
Results The patients were divided into the following four groups: those with the GGO pattern (group I, 13 patients), those with solid pattern and low FDG uptake (group II, 35 patients), those with solid pattern, high FDG uptake, and CEA <20 ng/ml (group III, 32 patients), and those with solid pattern, high FDG uptake, and CEA ≥20 ng/ml (group IV, 7 patients). The incidence of cell dedifferentiation, aggressiveness, and lymph node metastasis were significantly different among the groups ($p<0.0001$); . The 5-year disease-free survival rates were 100% in group I, 80.1% in group II, 43.7% in group III, and 16.7% in group IV ($p<0.0001$).
Conclusion Combined evaluation of preoperative FDG uptake, GGO, and serum CEA level may enable patients with T1 lung adenocarcinoma at low risk and at high risk of postoperative recurrence to be identified.

K. Higashi
Department of Radiology, Asanogawa General Hospital, Ishikawa, Japan

K. Higashi (✉) · T. Takahashi · H. Tonami
Department of Radiology, Kanazawa Medical University, 1-1, Daigaku, Uchinada, Kahokugun, Ishikawa 920-0293, Japan
e-mail: h550208@kanazawa-med.ac.jp

T. Sakuma
Department of Thoracic Surgery, Kanazawa Medical University, Ishikawa, Japan

K. Ito · T. Kato
Department of Biofunctional Research, National Institute for Longevity Sciences, Obu, Japan

S. Niho
Division of Thoracic Oncology, National Cancer Center Hospital East, Kashiwa, Japan

Y. Ueda
Department of Pathology, Kanazawa Medical University, Ishikawa, Japan

T. Kobayashi
Department of Radiology, Ishikawa Prefectural Hospital, Ishikawa, Japan

R. Sekiguchi
Division of Image Diagnosis, Tochigi Prefectural Cancer Center, Tochigi, Japan

Keywords Lung adenocarcinoma · Metastasis · Recurrence · FDG PET · GGO area · CEA level

Introduction

Lung cancer is the most common cause of mortality due to cancer worldwide. Non-small cell lung cancer (NSCLC) accounts for approximately 80% of lung cancers. Despite the potential benefits of surgical resection, patients with the same pathological stage of disease display marked variability in recurrence and survival. Moreover, the outcome after treatment in many cases is dismal. The poor results attained so far are, at least in part, related to the high potential of NSCLC to metastasize as well as to locally recur. These events, in turn, are not easy to predict. If the very high-risk patients could be identified before surgery, indications for intensive pre- or postoperative treatment, including radiotherapy and chemotherapy, could be determined, and if the very low-risk patients could be identified before surgery, appropriate surgical treatment, especially less-invasive surgical intervention, could be planned.

Better knowledge of the molecular biology or morphology of NSCLC might improve our ability to predict the outcome for any individual patient, which in turn would help to define subgroups of patients for adjuvant treatment or for less-invasive surgical intervention. Recently, FDG uptake in NSCLC has been correlated with the growth rate and proliferative capacity of the tumour [1] and has also been identified as an independent prognostic factor correlated with tumour aggressiveness [2] and survival [3–5] in patients with lung cancer. The more metabolically active the tumour, the more aggressive it is and the worse the outcome. CT findings, especially the extent of ground-glass opacity (GGO) within the tumour, are also inversely correlated with aggressiveness and survival in patients with lung adenocarcinoma [6–8]. The fewer GGO areas within the tumour, the more aggressive it is. Serum CEA level is also an independent prognostic factor in patients with NSCLC [9, 10].

On the basis of these findings, we determined FDG uptake, the extent of GGO, and the serum CEA level in patients with pulmonary adenocarcinoma of 3 cm or smaller. The aim of the study was to predict postoperative progonosis and histological features (dedifferentiation, aggressiveness, N factor) before surgery in small-sized pulmonary adenocarcinomas according to FDG uptake on PET, the extent of GGO on CT, and serum CEA levels, and to select not only a subgroup of very low-risk patients who could in the future benefit from a less-aggressive surgical procedure, but also a subgroup of very high-risk patients who could benefit from intensive preoperative treatment, including radiotherapy and chemotherapy.

Materials and methods

Patient preparation

This study was approved by the ethics committees of Kanazawa Medical University. The retrospective study included 87 consecutive patients (40 men, 47 women; mean age 64 years, age range 42–84 years) with lung adenocarcinoma of 3 cm or smaller who had undergone surgery between April 1997 and January 2005, and had been followed up to estimate local recurrence or distant metastasis. All patients underwent a lobectomy with hilar and mediastinal lymphadenectomy. Patients who underwent only a wedge resection of their lung cancer were excluded from this study, because the relapse rate in these patients is higher than that in patients who undergo a lobectomy with hilar and mediastinal lymphadenectomy. None of the patients had received neoadjuvant therapy prior to resection.

Imaging protocol

PET scanning was performed with one of the following dedicated PET cameras: a Headtome IV (Shimadzu, Kyoto, Japan), an Advance (General Electric Medical Systems, Milwaukee, WI), or an ECAT HR (Siemens/CTI PET Systems, Knoxville, TN). All patients fasted for 6 h before scanning. Blood was drawn for baseline blood glucose determination, and the data were recorded. FDG was administered intravenously. The average injection activity of FDG was 370 MBq. After an uptake period of 50–60 min, an emission scan was acquired. Two-dimensional acquisition was used in two of the PET centres, and three-dimensional acquisition was used in the third PET centre. Transmission scans were obtained in all subjects for attenuation correction. In two of the PET centres, filtered back-projection with measured attenuation correction was used for reconstruction. In the third PET centre, iterative reconstruction with segmented attenuation correction was used, applying the expectation maximization algorithm with ordered subsets (28 subsets and two iterations).

CT scanning was performed on an X-vision (Toshiba Medical Systems, Tokyo, Japan), an X-force (Toshiba Medical Systems), a Somatom Plus (Siemens Medical Systems, Erlangen, Germany), or a Sensation (Siemens Medical Systems) scanner. Routine scanning of the entire lung was first performed in the helical mode with a table speed of 10 mm/s and a section thickness of 10 mm. Additional thin sections of thickness 2.0 mm to image the tumour were acquired in all patients. CT images were reconstructed with a high spatial frequency algorithm and were printed with fixed window settings (lung centre −700 HU and width 1,500 HU).

Data analysis

FDG accumulation within the primary lung cancer on the attenuation-corrected images was graded. Two nuclear medicine doctors retrospectively analysed the PET findings. The readers were blind to the outcome, patient status, and the findings observed with the other modality. A two-point visual scoring system (low or high grade) was used to interpret the FDG uptake within the primary lesions: low grade was defined as activity less than or equal to that of the mediastinal blood pool, and high grade as activity greater than that of the mediastinal blood pool. This method is a modification of that used by Cheran et al. [11], and is the same method as previously reported [12]. Visual interpretation is sufficient for characterizing solitary pulmonary nodules, and quantitative analysis does not improve the accuracy [13, 14].

Two chest radiologists retrospectively analysed the CT findings on thin-section CT scans. The readers were blind to the outcome, patient status, and the findings observed with the other modality. The tumour contents were semiquantitatively classified according to the area occupied by GGO within the whole tumour. GGO was defined as a hazy and amorphous increased lung attenuation without obscuration of the underlying vascular markings and bronchial walls. The percentage of GGO area was calculated as $[(D_{GGO} - D)/D_{GGO}] \times 100$, where D_{GGO} is the greatest diameter of the tumour including the GGO area, and D is the greatest diameter of the tumour without the GGO area. The tumours were classified into two groups according to the area of GGO: less than 50% (solid pattern) and more than 50% (GGO pattern), using a method modified from that of Aoki et al. [7].

Serum CEA levels

We studied the effects of setting the serum CEA level threshold at 5, 10, and 20 ng/ml, and found that a threshold at 20 ng/ml was the best predictive parameter for disease-free survival calculated with the Kaplan-Meier method. The threshold for serum CEA level was fixed at 20 ng/ml. The patients were classified into those with a serum CEA level <20 ng/ml and those with a CEA level ≥20 ng/ml.

Clinical-pathologic correlation

A pathologist retrospectively analysed the histopathologic findings.

Histopathological features All 87 lung cancers were histopathologically proven to be primary lung adenocarcinoma. All surgical specimens were stained with haematoxylin and eosin, and elastica van Gieson stains. Cell dedifferentiation (bronchioloalveolar carcinoma, well-differentiated adenocarcinoma, or moderately/poorly differentiated adenocarcinoma), aggressiveness (positive or negative), pathological N factor (positive or negative) were evaluated in all surgical specimens. Vascular (blood and lymphatic vessels) invasion and pleural invasion were evaluated to estimate aggressiveness.

Tumour size The size of each of the 87 primary lesions was recorded as the largest diameter at surgical resection. All 87 lung cancers were histopathologically proven to be 3 cm or less than 3 cm in size.

Table 1 Patient and tumour characteristics

Characteristic	No. (%) of patients
Age (years)	
≤65	43 (49.4)
>65	44 (50.6)
Gender	
Male	40 (46.0)
Female	47 (54.0)
GGO	
GGO pattern	13 (14.9)
Solid pattern	74 (85.1)
FDG uptake	
Low	47 (54.0)
High	40 (46.0)
Serum CEA level (ng/ml)	
<20	80 (92.0)
≥20	7 (8.0)
Tumour size (cm)	
≤1	5 (5.7)
1.1–2	39 (44.8)
2.1–3	43 (49.5)
Clinical stage	
IA	72 (82.8)
IIA	2 (2.3)
IIIA	13 (14.9)
Pathological stage	
IA	68 (78.2)
IB	4 (4.6)
IIA	3 (3.4)
IIB	0 (0)
IIIA	10 (11.5)
IIIB	2 (2.3)
Dedifferentiation	
Bronchioloalveolar carcinoma	15 (17.2)
Well-differentiated adenocarcinoma	43 (49.5)
Moderately/poorly differentiated adenocarcinoma	29 (33.3)
Aggressiveness	
Negative	55 (63.2)
Positive	32 (36.8)
Lymph node involvement	
Negative	72 (82.8)
Positive	15 (17.2)
Recurrence	
Negative	69 (79.3)
Positive	18 (20.7)

Pathological stage Pathological results were used assign a final pathological stage according to the revised international system for staging lung cancer [15].

Disease-free survival data Follow-up consisted of clinical and radiological examination every 6 months in the first 2 years after surgery, then once a year; clinical and radiological examination was carried out after surgery. We chose to evaluate the time to relapse considering either local recurrence or distant metastasis. Cancer recurrence was defined as the period ranging from the date of surgery to the date when a relapse was diagnosed. An observation was censored at the last follow-up if the patient was alive.

Statistical analysis

Statistical analysis was performed using the SPSS software system (SPSS for Windows, version 10.0; SPSS, Chicago, IL). Multivariate analysis was performed with the Cox proportional hazards model to assess the joint effects and interactions of the variables on disease-free survival. An exact χ^2 test was used to evaluative the relationship between histopathological findings, risk of recurrence, and PET, CT and CEA level results. Disease-free survival was calculated using the Kaplan-Meier method, and groups were compared using the log-rank test. The intra- and interobserver variabilities of each method were determined using the kappa statistics for visual scores according to FDG uptake and for groups according to the area of GGO. The level of significance was $p<0.05$.

Results

The patient and tumour characteristics are shown in Table 1.

Clinical-pathological correlation

The patients were divided into the following four groups: those with the GGO pattern (group I, 13 patients), those with the solid pattern and low FDG uptake (group II, 35 patients), those with the solid pattern, high FDG uptake, and CEA <20 ng/ml (group III, 32 patients), and those with the solid pattern, high FDG uptake, and CEA ≥20 ng/ml (group IV, 7 patients) (Table 2). The incidence of cell dedifferentiation, aggressiveness, and lymph node metastasis were significantly different among the groups ($p<0.0001$). No patient with the GGO pattern on the CT scan had a high FDG uptake on the PET scan or a CEA ≥20 ng/ml. In group I, cell dedifferentiation, aggressiveness, and lymph node metastasis were not seen. In contrast, the incidence of cell dedifferentiation, aggressiveness, and lymph node metastasis were highest in group IV.

Disease-free survival data

Of the 87 patients, 18 (20.7%) suffered a recurrence during follow-up at a median time of 11 months after surgery. The time to recurrence varied between 2 and 47 months. The remaining 69 patients had not suffered a recurrence at the time of data analysis. Follow-up for these patients was available for a median period of 18 months after surgery.

Multivariate analysis was performed with the Cox proportional hazards model to assess the joint effects and interactions of the variables on disease-free survival. In 13 patients with the GGO pattern on CT, recurrence was not seen. Therefore, in 74 patients with the solid pattern on CT, we performed a multivariate analysis. Age (≤65 or >65 years), gender (male or female), FDG uptake (high or low), and serum CEA level (<20 or ≥20 ng/ml) were selected as parameters. Both FDG uptake and serum CEA level were independent parameters in patients with a solid pattern on the CT scan ($p=0.009$ and $p=0.032$, respectively).

Table 2 Risk of dedifferentiation, aggressiveness, and lymph node involvement based on GGO pattern, FDG uptake, and serum CEA level (numbers in parentheses are percentages)

Group		Dedifferentiation			Aggressiveness[a]		Lymph node involvement	
		Bronchioloalveolar carcinoma	Well-differentiated adenocarcinoma	Moderately/poorly differentiated adenocarcinoma	Negative	Positive	Negative	Positive
I	GGO	6 (46.2)	7 (53.8)	0 (0)	13 (100)	0 (0)	13 (100)	0 (0)
II	Solid, low FDG	8 (22.9)	23 (65.7)	4 (11.4)	29 (82.9)	6 (17.1)	33 (94.3)	2 (5.7)
III	Solid, high FDG, CEA <20 ng/ml	1 (3.1)	12 (37.5)	19 (59.4)	13 (40.6)	19 (59.4)	25 (78.1)	7 (21.9)
IV	Solid, high FDG, CEA ≥20 ng/ml	0 (0)	1 (14.3)	6 (85.7)	0 (0)	7 (100)	1 (14.3)	6 (85.7)

[a] Vascular invasion and/or pleural invasion.

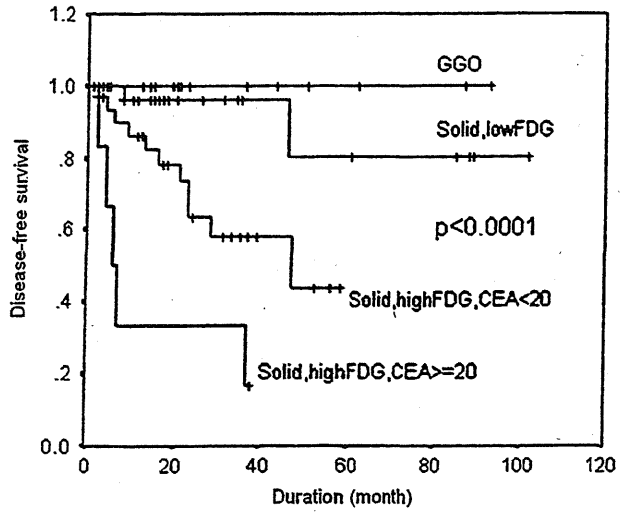

Fig. 1 Disease-free survival in four groups of patients (n=87) with T1 lung adenocarcinoma: 13 patients with the GGO pattern on CT (group I), 35 patients with solid pattern on CT and low FDG uptake on PET (group II), 32 patients with solid pattern on CT, high FDG uptake on PET, and CEA <20 ng/ml (group III), and 7 patients with solid pattern on CT, high FDG uptake on PET, and CEA ≥20 ng/ml (group IV). Disease-free survival was calculated using the Kaplan-Meier method, and the groups were compared using the log-rank test. The disease-free survival rates were significantly different among the four groups (p<0.0001)

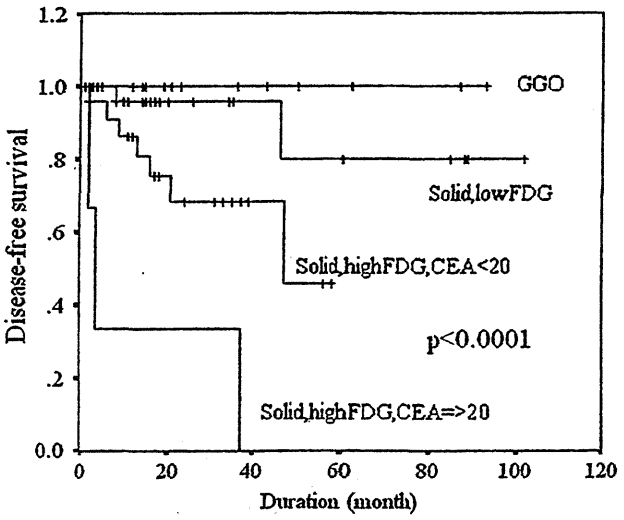

Fig. 2 Disease-free survival in four groups of patients (n=72) with clinical stage IA (T1N0M0) lung adenocarcinoma: 12 patients with GGO pattern on CT (group I), 33 patients with solid pattern on CT and low FDG uptake on PET (group II), 23 patients with solid pattern on CT, high FDG uptake on PET, and CEA <20 ng/ml (group III), and 4 patients with solid pattern on CT, high FDG uptake on PET, and CEA ≥20 ng/ml (group IV). Disease-free survival was calculated using the Kaplan-Meier method, and the groups were compared using the log-rank test. The disease-free survival rates were significantly different among the four groups (p<0.0001)

The 5-year disease-free survival rates were 100% in group I (GGO pattern on CT), 80.1% in group II (solid pattern on CT and low FDG uptake on PET), 43.7% in group III (solid pattern on CT, high FDG uptake on PET, and CEA <20ng/ml), and 16.7% in group IV (solid pattern on CT, high FDG uptake on PET, and CEA ≥20 ng/ml), and the disease-free survival rates were significantly different among the four groups (p<0.0001; Fig. 1). In the patients with clinical stage IA or pathological stage IA lung adenocarcinoma, the disease-free survival rates were also significantly different among the four groups (p<0.0001, p=0.0001, respectively; Figs. 2 and 3). Representative cases are shown in Figs. 4, 5, 6 and 7.

Intra- and interobserver reproducibilities

The kappa statistics for intra- and interobserver reproducibilities in visual scoring of FDG uptake (low or high) were 0.87 and 0.83, respectively, indicating good agreement, and in classifying the area of GGO (GGO pattern or solid pattern) were 0.75 and 0.72, respectively, also indicating good agreement.

Discussion

The principal finding of this study was that combined evaluation of preoperative GGO area on CT, FDG uptake

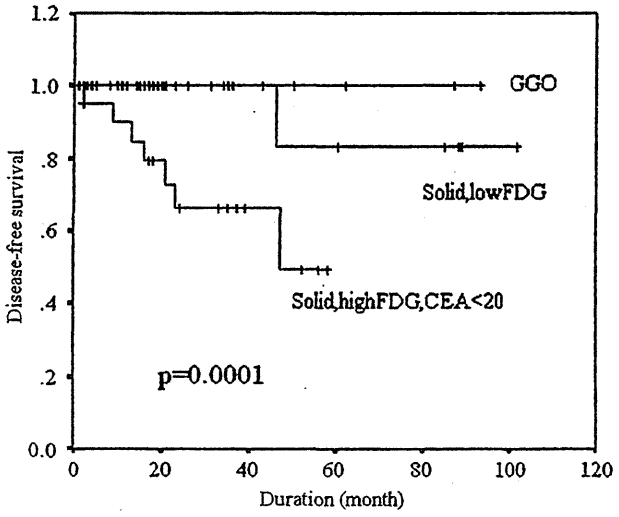

Fig. 3 Disease-free survival in four groups of patients (n=68) with pathological stage IA (T1N0M0) lung adenocarcinoma: 13 patients with GGO pattern on CT (group I), 33 patients with solid pattern on CT and low FDG uptake on PET (group II), and 21 patients with solid pattern on CT, high FDG uptake on PET, and CEA <20 ng/ml (group III). Disease-free survival was calculated using the Kaplan-Meier method, and the groups were compared using the log-rank test. Group IV (solid pattern on CT, high FDG uptake on PET, and CEA ≥20 ng/ml) is not shown because there was only one patient in this group. The disease-free survival rates were significantly different among the four groups (p=0.0001)

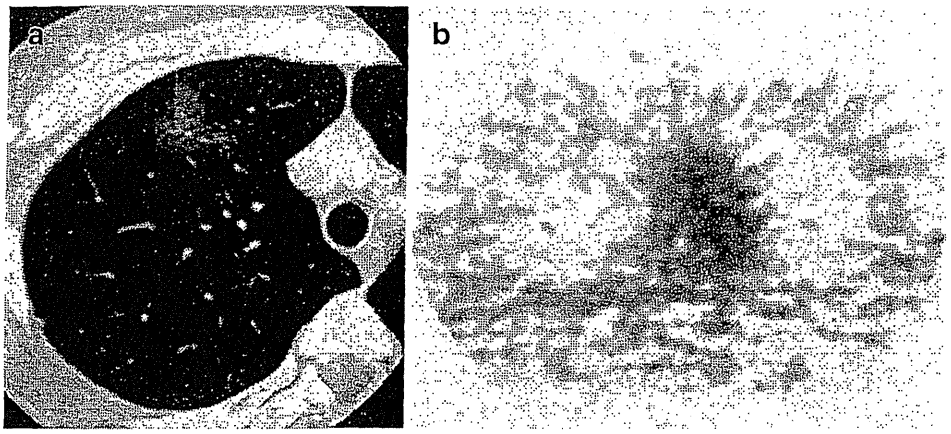

Fig. 4 A patient in group I: **a** CT image shows the GGO pattern; **b** PET image shows low FDG uptake. Cell dedifferentiation, aggressiveness, and lymph node metastasis were not seen. The patient showed no recurrence over a period of 93 months after surgery

on PET, and serum CEA level may enable patients with highly invasive lung adenocarcinomas with a poor prognosis to be indentified. For example, the 5-year disease-free survival rate was 16.7% for patients with surgically resected T1 lung adenocarcinoma with the solid pattern on CT, high FDG uptake on PET, and a high CEA level (≥20 ng/ml), but 80.1% for patients with the solid pattern on CT and low FDG uptake on PET.

These findings can be explained by the fact that the greater the FDG uptake, the higher the malignancy grade. FDG is avidly taken up by tumour cells because cancer tissue consumes a large amount of glucose as an energy source. FDG uptake reflects cell dedifferentiation [16], proliferative potential [1], aggressiveness [2], and prognosis [3–5] in patients with lung cancer. Cheran et al. have also reported that lung cancers with negative PET findings are associated with a favourable prognosis [11]. These findings are compatible with our current results.

The patients with high FDG uptake lung adenocarcinoma were classified into two groups, those with a low CEA level (<20 ng/ml) group and those with a high CEA level (≥20 ng/ml). The incidence of cell dedifferentiation, aggressiveness, lymph node metastasis, and recurrence were high in the group with high CEA levels (≥20 ng/ml). Several studies have shown that preoperative high serum CEA levels are associated with poor survival after surgical resection in lung cancer [9, 10, 17, 18]. These findings are also compatible with our current results.

In this study, 20.7% of patients with resected T1 lung adenocarcinoma presented with tumour recurrence. The ability to predict recurrence is an important contribution to treatment planning. If the postoperative prognosis can be determined before surgery, indications for intensive pre- or postoperative treatment, including radiotherapy and chemotherapy, can be determined, and appropriate surgical treatment, especially less-invasive surgical intervention, can be planned. Thus, FDG PET appears to be useful in determining the optimal therapeutic policy and in contributing to improving the postoperative prognosis. For example, the West Japan Study Group for Lung Cancer Surgery examined the efficacy of an oral 5-fluorouracil derivative as a postoperative adjuvant therapy for pathological stage I NSCLC [19], and concluded that postoperative adjuvant therapy might be effective in patients with pathological stage IA (T1N0M0) adenocarcinoma.

In our study, high FDG uptake identified a subgroup of patients with the worst prognosis for recurrence, and this parameter seemed to be more important in stage IA disease.

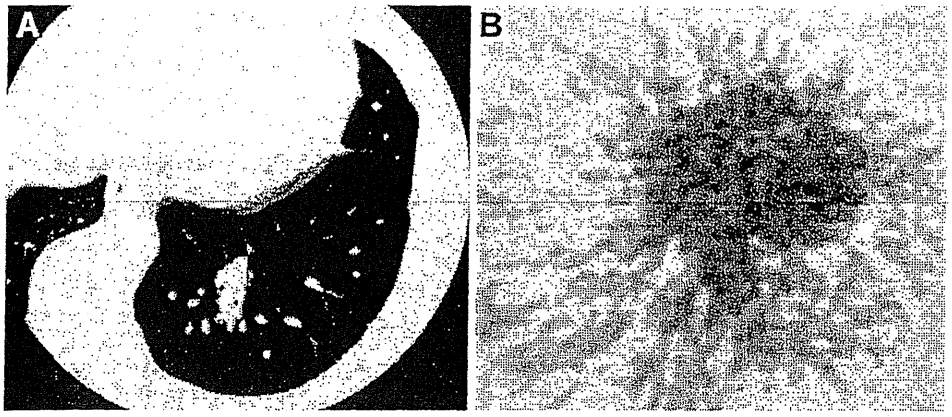

Fig. 5 A patient in group II: **a** CT image shows the solid pattern; **b** PET image shows low FDG uptake. Cell dedifferentiation, aggressiveness, and lymph node metastasis were not seen. The patient showed no recurrence over a period of 85 months after surgery

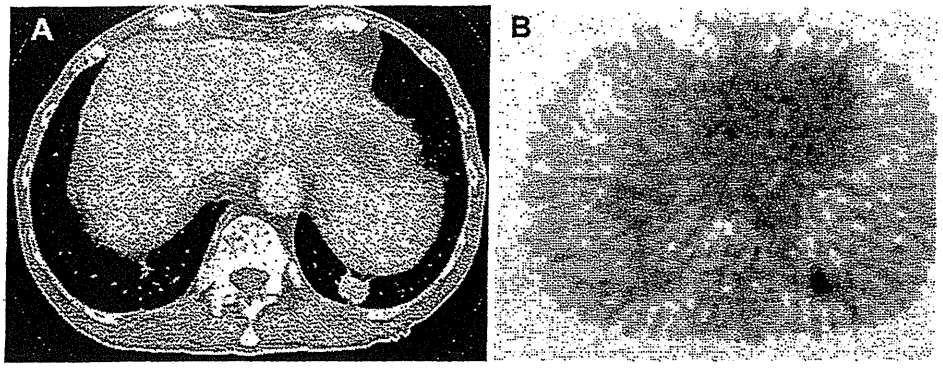

Fig. 6 A patient in group III: **a** CT shows the solid pattern; **b** PET image shows high FDG uptake. The CEA level was 3.6 ng/ml. Cell dedifferentiation, and aggressiveness (vascular invasion) were seen. The patient showed recurrence 2 months after surgery

Therefore, it is suggested that patients with hypermetabolic lesions may benefit more from pre- or postoperative adjuvant therapy. As another example, in a prospective randomized trial comparing limited resection with lobectomy for the management of patients with clinical T1N0 [20], the limited resection group had a significantly higher recurrence rate than the lobectomy group. The authors therefore concluded that limited resection cannot be recommended as the resection of choice for patients with T1N0 disease. Ichinose et al. [21] reported that 44% of tumours showed intratumoral vessel invasion in patients with resected NSCLC classified as pathological stage I located on the periphery of the lung. They speculated that this was the main reason that the limited resection group had a higher recurrence rate. Others have reported that intratumoral vessel invasion is correlated with a poor prognosis in patients with NSCLC [22, 23].

Therefore, if we could select patients with tumours without aggressiveness, and if we could select patients with a low risk of relapse and were able to predict relapse, limited resection might be successfully performed without recurrence. In our series, clinical stage IA tumours with the GGO pattern on CT or low FDG uptake on PET had a low rate of relapse, and clinical stage IA tumours with high FDG uptake on PET in patients with a high serum CEA level (≥20 ng/ml) had a high rate of relapse. These findings suggest that combined evaluation of preoperative GGO area on CT, FDG uptake on PET, and serum CEA level is important when planning appropriate surgical treatment, especially less-invasive surgical intervention. Limited resection might be successfully performed without recurrence in patients with the GGO pattern or low FDG uptake lung cancer.

It has been reported that the proportion of GGO areas on thin-section CT scans is a strong predictor of recurrence and survival in patients with clinical T1N0M0 adenocarcinoma [6–8], and thus could be a useful index for planning a limited surgical resection in these patients [24]. A greater extent of GGO in a nodule correlates with improved prognosis. We found that the GGO area were well correlated with histological prognostic factors, such as vascular invasion and pleural invasion, and were well correlated with the risk of recurrence. The incidence of vascular invasion and pleural invasion, and the risk of recurrence in lung adenocarcinomas with the GGO pattern were significantly lower than in those with the solid pattern. The patients with the GGO pattern had a significantly better prognosis. These results are compatible with findings reported previously [6–8, 24].

Kim et al. [6] have reported that the extent of GGO in a nodule is greater in bronchioloalveolar carcinomas than in other adenocarcinomas and a greater extent of GGO correlates with an improved prognosis. Bronchioloalveolar carcinoma is, however, classified into three histological subtypes (goblet cell, Clara cell, and type 2 pneumocyte), and the Clara cell subtype shows the solid but not the GGO

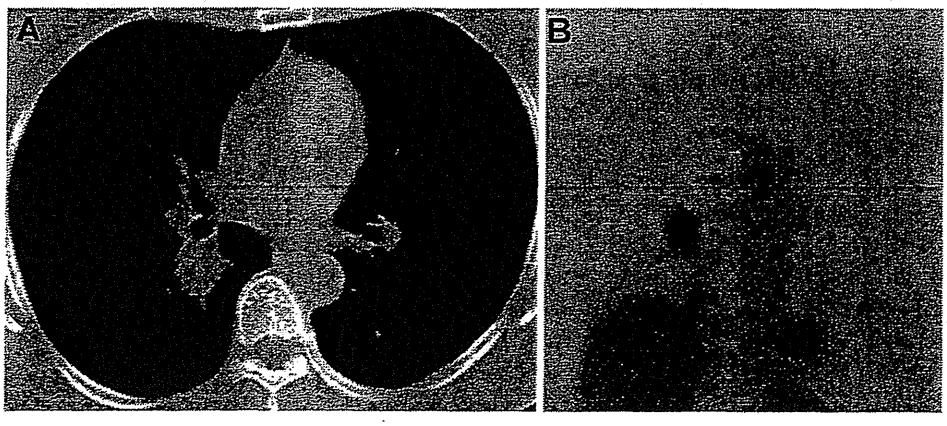

Fig. 7 A patient in group IV: **a** CT image shows the solid pattern; **b** PET image shows high FDG uptake. The CEA level was 142 ng/ml. Cell dedifferentiation, aggressiveness (vascular invasion), and lymph node involvement were seen. The patient showed recurrence 4 months after surgery

pattern [25]. In our study, some bronchioloalveolar carcinomas showed the solid pattern on CT (Table 2). Therefore, some of the patients with lung adenocarcinoma with the solid pattern on CT had a favourable prognosis. In our study, there were also two groups of patients with lung adenocarcinoma and the solid pattern on CT, a relapse group and a non-relapse group. Among the patients with lung adenocarcinoma with the solid pattern on CT, the risk of recurrence in those with high FDG uptake was significantly higher than in those with low FDG uptake. Therefore, FDG uptake had significant value in predicting increased relapse in lung adenocarcinomas with the solid pattern on CT.

However, this study had limitations. First, a visual scoring system was used to interpret the FDG uptake within the primary lesions. Visual interpretation is, however, sufficient for characterizing solitary pulmonary nodules, and quantitative analysis does not improve the accuracy [13, 14]. Second, this was a multicentre study with large variations in the capacity of the machines and the image processing. It has been reported that SUV measurements are affected by the applied method for both image reconstruction and attenuation correction [26, 27]. Furthermore, it is uncertain whether and to what degree the geometry and specifications of different PET tomographs from different manufacturers might affect the accuracy and reproducibility of SUV measurements [27]. For these reasons, a visual grading system was used to interpret FDG uptake within the primary lesions, and the SUV threshold was not used. Third, the extent of GGO was derived from a crude linear estimate that ignored tumour shape and may not have truly depicted the percentage area of GGO. The diameter measure is meaningless for nonspherical tumours. More importantly, the ratio of diameters is not linearly related to the true volume ratio. However, our method modified from that of Aoki et al. [7] was simple, and intra- and interobserver reproducibilities were excellent.

The current results suggest that the combination of FDG uptake on PET, GGO area on CT, and serum CEA level may provide accurate information regarding risk of vascular invasion, pleural invasion, lymph node metastasis, and recurrence in clinical settings in which limited surgical resection or adjuvant therapy is desirable. Further studies assessing patient survival after limited surgical resection are recommended.

Conclusions

In patients with T1 lung adenocarcinoma, combined evaluation of preoperative FDG uptake, GGO area, and serum CEA level may enable patients at a low and at a high risk of postoperative recurrence to be identified. Our observations are of potential interest for the development of rational pre- or postresection treatment strategies based on the estimated risk of recurrence of patients with surgically resected T1 lung adenocarcinoma.

Acknowledgements This work was supported by a Grant for Project Research from the High-Technology Center of Kanazawa Medical University (H2008-12, H2007-12, H2007-10, S2006-2, S2005-6), by a Grant-in-Aid for Cancer Research (16-5) from the Ministry of Health and Welfare, Japan, and by a Grant-in-Aid (19590370) for scientific research from the Ministry of Education.

Conflicts of interest statement None.

References

1. Tann M, Sandrasegaran K, Winer-Muram HT, Jennings SG, Welling ME, Fletcher JW. Can FDG-PET be used to predict growth of stage I lung cancer? Clin Radiol 2008;63:856–63.
2. Okada M, Tauchi S, Iwanaga K, Mimura T, Kitamura Y, Watanabe H, et al. Associations among bronchioloalveolar carcinoma components, positron emission tomographic and computed tomographic findings, and malignant behavior in small lung adenocarcinomas. J Thorac Cardiovasc Surg 2007;133:1448–54.
3. Vansteenkiste J, Fischer BM, Dooms C, Mortensen J. Positron-emission tomography in prognostic and therapeutic assessment of lung cancer: systemic review. Lancet Oncol 2004;5:531–40.
4. Hanin FX, Lonneux M, Cornet J, Noirhomme P, Coulon C, Distexhe J, et al. Prognostic value of FDG uptake in early stage non-small cell lung cancer. Eur J Cardiothorac Surg 2008;33:819–23.
5. Sasaki R, Komaki R, Macapinlac H, Erasmus J, Allen P, Forster K, et al. [18F]fluorodeoxyglucose uptake by positron emission tomography predicts outcome of non-small-cell lung cancer. J Clin Oncol 2005;23:1136–43.
6. Kim EA, Johkoh T, Lee KS, Han J, Fujimoto K, Sadohara J, et al. Quantification of ground-grass opacity on high-resolution CT of small peripheral adenocarcinoma of the lung: pathologic and prognostic implications. AJR Am J Roentgenol 2001;177:1417–22.
7. Aoki T, Tomoda Y, Watanaba H, Nakata H, Kasai T, Hashimoto H, et al. Peripheral lung adenocarcinoma: correlation of thin-section CT findings with histologic prognostic factors and survival. Radiology 2001;220:803–9.
8. Matsuguma H, Nakahara R, Anraku M, Kondo T, Tsuura Y, Kamiyama Y, et al. Objective definition and measurement method of ground-glass opacity for planning limited resection in patients with clinical stage IA adenocarcinoma of the lung. Eur J Cardiothorac Surg 2004;25:1102–6.
9. Tomita M, Matsuzaki Y, Shimizu T, Hara M, Ayabe T, Onitsuka T. Serum carcinoembryonic antigen level in pN1 non-small cell lung cancer patients. Anticancer Res 2005;25:3601–5.
10. Matsuguma H, Nakahara R, Igarashi S, Ishikawa Y, Suzuki H, Miazawa N, et al. Pathologic stage I non-small cell lung cancer with high levels of preoperative serum carcinoembryonic antigen: clinicopathologic characteristics and prognosis. J Thorac Cardiovasc Surg 2008;135:44–9.
11. Cheran SK, Nielsen ND, Patz EF. False-negative findings for primary lung tumors on FDG positron emission tomography: staging and prognostic implications. AJR Am J Roentgenol 2004;182:1129–32.
12. Higashi K, Ito K, Hiramatsu Y, Ishikawa T, Sakuma T, Matsunari I, et al. 18F-FDG uptake by primary tumor as a predictor of intratumoral lymphatic vessel invasion and lymph node involvement in non-small cell lung cancer: analysis of a multicenter study. J Nucl Med 2005;46:267–73.

13. Nomori H, Watanabe K, Ohtsuka T, Naruke T, Suemasu K, Uno K. Visual and semiquantitative analysis for F-18 fluorodeoxyglucose PET scanning in pulmonary nodules 1 cm to 3 cm in size. Ann Thorac Surg 2005;79:984–8.
14. Kim SK, Allen-Auerbach M, Goldin J, Fueger BJ, Dahlbom M, Brown M, et al. Accuracy of PET/CT in characterization of solitary pulmonary lesions. J Nucl Med 2007;46:214–20.
15. Mountain CF. Revisions in the International System for Staging Lung Cancer. Chest 1997;111:1710–7.
16. Higashi K, Ueda Y, Seki H, Yuasa K, Oguchi M, Noguchi T, et al. Fluorine-18-FDG PET imaging is negative in bronchioloalveolar lung carcinoma. J Nucl Med 1998;39:1016–20.
17. Takamochi K, Yoshida J, Nishimura M, Yokose T, Sasaki S, Nishiwaki Y, et al. Prognosis and histologic features of small pulmonary adenocarcinoma based on serum carcinoembryonic antigen level and computed tomographic findings. Eur J Cardiothorac Surg 2004;25:877–83.
18. Sakao Y, Nakazono T, Sakuragi T, Natsuaki M, Itoh T. Predictive factors for survival in surgically resected clinical IA peripheral adenocarcinoma of the lung. Ann Thorac Surg 2004;77:1157–61.
19. Nakagawa M, Tanaka F, Tsubota N, Ohota M, Takao M, Wada H. A randomized phase III trial of adjuvant chemotherapy with UFT for completely resected pathological stage I non-small-call lung cancer: the West Japan Study Group for Lung Cancer Surgery (WJSG) – the 4th study. Ann Oncol 2005;16:75–80.
20. Ginsberg RJ, Rubinstein LV. Randomized trial of lobectomy versus limited resection for T1 N0 non-small cell lung cancer. Lung Cancer Study Group. Ann Thorac Surg 1995;60:615–22.
21. Ichinose Y, Yano T, Yokoyama H, Inoue T, Asoh H, Katsuda Y. The correlation between tumor size and lymphatic vessel invasion in resected peripheral stage I non-small cell lung cancer: a potential risk of limited resection. J Thorac Cardiovasc Surg 1994;108:684–6.
22. Roberts TE, Hasleton PS, Musgrove C, Swindell R, Lawson RA. Vascular invasion in non-small lung carcinoma. J Clin Pathol 1992;45:591–3.
23. Maeshima AM, Niki T, Maeshima A, Yamada T, Kondo H, Matsuno Y. Modified scar grade: a prognostic indicator in small peripheral lung adenocarcinoma. Cancer 2002;95:2546–54.
24. Nakamura H, Saji H, Ogata A, Saijo T, Okada S, Kato H. Lung cancer patients showing pure ground-glass opacity on computed tomography are good candidates for wedge resection. Lung Cancer 2004;44:61–8.
25. Mihara N, Ichikado K, Johkoh T, Honda O, Higashi M, Tomiyama N, et al. The subtypes of localized bronchioloalveoalar carcinoma: CT-pathologic correlation in 18 cases. AJR Am J Roentgenol 1999;173:75–9.
26. Ramos CD, Erdi YE, Gonen M, Riedel E, Yeung HW, Macapinlac HA, et al. FDG-PET standardized uptake values in normal anatomical structures using iterative reconstruction segmented attenuation correction and filtered back-projection. Eur J Nucl Med Mol Imaging 2001;28:155–64.
27. Schoder H, Erdi YE, Chao K, Gonen M, Larson SM, Yeung HW. Clinical implications of different image reconstruction parameters for interpretation of whole-body PET studies in cancer patients. J Nucl Med 2004;45:559–66.

12 for the Beginners 造影MRIの意義 Revisited

Contrast Enhanced MRI

胸部

12. 乳腺

河野　晶子　栃木県立がんセンター画像診断部／臨床検査部病理診断科
黒木　嘉典／吉田　慶之／山邉裕一郎
山本　孝信／関口　隆三　栃木県立がんセンター画像診断部
黒木　聖子　国立がんセンターがん予防・検診研究センター

乳腺領域において，MRIは必須の検査となっている。主な目的は，ハイリスク群のサーベイランスから，日常臨床の良悪性鑑別，術前画像診断では進展範囲や多発病巣の評価などである。最近では，術前化学療法（neoadjuvant chemotherapy：NAC）の治療効果判定にも用いられている。この乳腺MRI検査の中で，中心的な役割を果たすのは造影MRIである。本稿では，1.5T MRI装置における乳腺の造影MRIについて，撮像法と代表症例について概説する。

乳腺造影MRIの歴史と現状

乳腺MRIの適応は，2006年改訂の米国放射線学会（American College of Radiology：ACR）のガイドラインには12項目が挙げられている（表1）[1]。わが国における乳腺MRIは，主に術前の腫瘍進展度範囲診断に用いられてきたが，より進んだ欧米では，適応が非常に広く考えられていることがわかる。

乳腺MRIの中心は，造影検査である。乳腺の造影MRIの報告は，1986年のHeywangらが最初である[2]。この時点では，スライス厚5mm，撮像時間は5分程度であった。それから3年後の1989年に，現在のダイナミックスタディの原型がKaiserらによって報告された[3]。空間分解能よりも時間分解能を優先させた撮像法で，60秒撮像を10回繰り返す方法である。その後，主に欧州からダイナミックスタディの有用性が報告され[4),5]，次いで，造影パターンをより詳細にとらえることができるダイナミックカーブの重要性が認識され，診断手法として確立した[6]。

一方，米国での乳腺MRIは，血流動態評価よりも形態診断を重要視して発達してきている[7),8]。撮像法は空間分解能を重要視する片側撮像（患側矢状断）が基本であった。

このように，乳腺造影MRIの黎明期には2つの大きな潮流があったが，近年のMRIの進歩により，高時間分解能と高空間分解能の両方を同時に達成することが可能となり，診断において乳腺ダイナミック造影MRIは最重要な地位を占めるようになった。そこで，以下に造影前と造影後（早期相，遅延相）のセミ・ダイナミックスタディもダイナミックスタディに含めて，その有用性について述べる。

乳腺MRIの撮像プロトコール

図1，2に，当院における乳腺MRIの撮像プロトコールとダイナミックスタディの撮像条件を示す。使用するコイルは，通常の乳腺専用コイルではなく，表面コ

表1　ACRのガイドラインにおける乳腺MRIの現在の適応

1. Lesion characterization
2. Neoadjuvant chemotherapy
3. Infiltrating lobular carcinoma
4. Infiltrating ductal carcinoma
5. Axillary adenopathy, primary unknown
6. Postoperative tissue reconstruction
7. Silicone and nonsilicone breast augmentation
8. Invasion deep to fascia
9. Contralateral breast examination in patients with breast malignancy
10. Postlumpectomy for residual disease
11. Surveillance of high-risk patients
12. Recurrence of breast cancer

〈0913-8919/09/¥300/ 論文 /JCLS〉

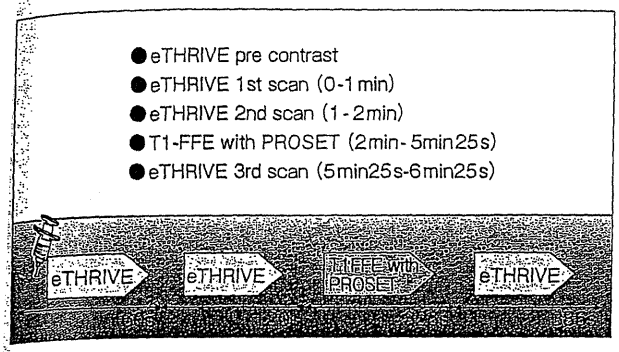

図1　当院における乳腺造影MRIプロトコール

●STIR：Bil.axial, 3min6s
●SPAIR-DWI：Bil.axial, 2min28s
b factor 0, 500, 1000, 1500, 2000
TR/TE 5702/84, NSA 2
●T1WI w/o Fat Suppression：Bil.axial, 1min36s
●3D-Dynamic study：Bil.axial, 1min×4
Actual voxel size 1mm×1mm×2mm
Recon. voxel size 1mm×1mm×1mm
●High resolution T1FFE w/ PROSET：Lateral Sag., 3min25s
Actual voxel size 0.52mm×0.68mm×2mm
Recon. voxel size 0.29mm×0.29mm×1mm
●MRS：about 10min

図2　当院における乳腺MRIの撮像条件
使用装置：Achieva 1.5T R2.5.3（フィリップス社製）
使用コイル：Flex Sコイルと Flex Mコイルを使用
造影剤：Gd-DTPA製剤（0.2mL/kg）
ダイナミック施行時は，自動注入器を用いて2mL/sで注入後，生理食塩水20mLを同速度でフラッシュ。

a：THRIVE

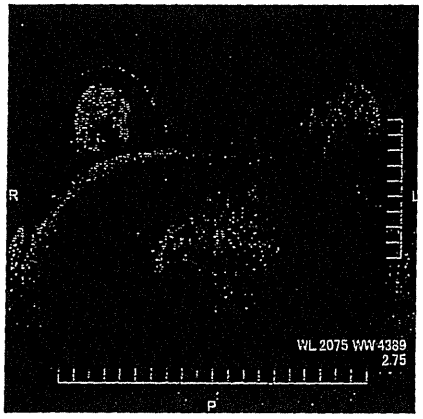

b：eTHRIVE

図3　同位置症例のNAC前後におけるeTHRIVEとTHRIVEの脂肪抑制効果の比較

イルであるFlex Sコイルと Flex Mコイルを使用し，4 channel dual surface coil systemにて撮像している。撮像の中心はダイナミックスタディで，ACRのBI-RADS（Breast Imaging Reporting and Data System）-MRIを念頭に置いている[1]。造影剤は通常のガドリニウム造影剤を規定量使用している。あらかじめ静脈注射用ラインを前腕から確保した後，自動注入器で2mL/sの注入速度で静注し，その後生理食塩水15mLで後押しをしている。ダイナミックスタディは両側乳房をターゲットにし，シーケンスは3D撮像法であるeTHRIVEに脂肪抑制法のSPAIRを組み合わせている。eTHRIVEはZ軸方向にもlinear filling orderが可能であり，これにSPAIRを組み合わせることで，従来よりも効果的に脂肪抑制効果を得ることができる（図3）。空間分解能は，撮像面内が1mm×1mm，スライス厚は2mmで，実際の画像は1mm×1mm×1mmのアイソトロピック・ボクセルとし，矢状断と冠状断のMPR（multiplanar reconstruction）像を作成している。ダイナミックスタディ1回の撮像時間は1分で，造影剤注入開始から2分以内に2回撮像し，約5～6分後から，delayed slopeのために3回目の撮像を行っている。

2分以内に2回撮像を行ってinitial slopeを決定しているが，initial slopeを決定するためだけであれば2回の撮像は必要ない。1分以内の画像は，いわゆるfaint enhancement対策である。若年者や乳腺症が強い症例では，背景乳腺も造影効果が亢進しており，2分前後には病変と同程度に造影されることが経験される。このような症例で病変と背景乳腺を鑑別するために，造影剤注入開始1分以内の画像が有用である。

もちろん形態診断も重要である。造影2回目から3回目にかけての約3分30秒間は，ある意味「自由時間」であり，当院では空間分解能を重視した片側乳房の高精細画像の撮像に利用している。撮像シーケンスはT1FFEにPROSETを併用し，撮像面内を0.52mm×0.68mm×2mm，実際の画像は0.29mm×0.29mm×1mmで作成している。高精細画像に求められる空間分解能はどの程度かということについてはまだコンセンサスが得られておらず，当院の設定が推奨されるかどうかは疑問の余地も残る。もう少し空間分解能を落として両側乳房を撮像するべきかもしれない。

これらダイナミックスタディと高精細画像の一連の造影MRIの前後に，脂肪抑制併用T2強調像（またはSTIR），脂肪抑制のないT1強調像，拡散強調画像（DWI），MRスペクトロスコピー（MRS）を撮像している。撮像時間は30分以内である。

症例—1　浸潤性乳管癌（図4）

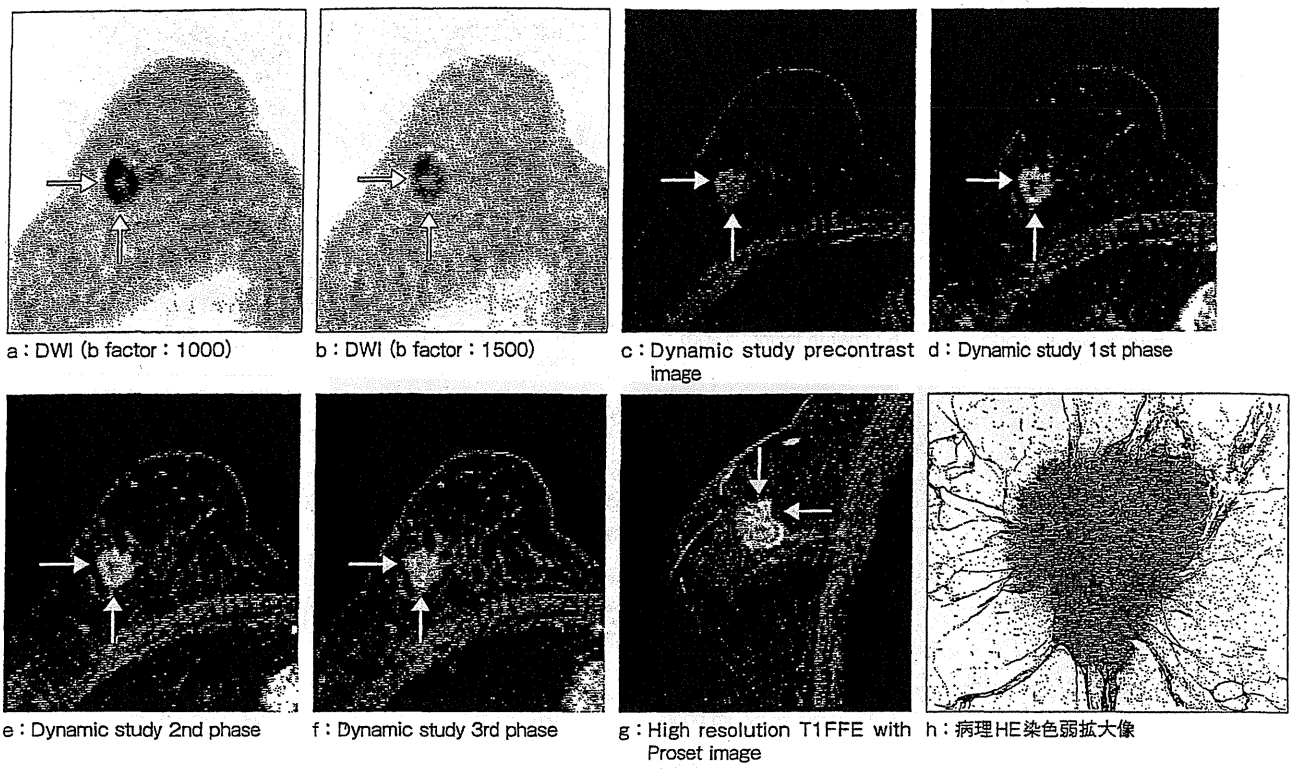

a：DWI (b factor：1000)　b：DWI (b factor：1500)　c：Dynamic study precontrast image　d：Dynamic study 1st phase

e：Dynamic study 2nd phase　f：Dynamic study 3rd phase　g：High resolution T1FFE with Proset image　h：病理HE染色弱拡大像

図4　症例1：浸潤性乳管癌（65歳，女性）

造影MRIの読影

ダイナミックスタディは，血流情報の解析に他ならない。そのため，造影MRIの読影は，造影剤急速静注後2～3分までのinitial slopeと，5～6分後以降（あるいは8分後まで）のdelayed slopeの組み合わせで画像を解釈する手法であると言える。以前から欧州で広く使われているGöttingen scoreやMARIBS（Magnetic Resonance Imaging in Breast Screening）のscoring systemが有名であるが，今後はACRのBI-RADS-MRIに準拠した読影が望ましい[9),10)]。

initial slopeによって病変の早期濃染の程度を3つに分類する。早期濃染は，造影前後の信号強度の差を，造影前の信号強度で除した百分率で定義される。Göttingen scoreを用いることが多く，50％未満の場合はslow，50～100％がmedium，100％より大きい場合はrapidと分類される。

delayed slopeは，persistent，plateau，washoutに分類されるが，BI-RADS-MRIでは明確な定義はなされていない。Göttingen scoreを参考にすると，persistentが10％を超える増加，plateauが10％以内の増減，washoutが10％を超える減少となる。これらの分類を用いた良悪性鑑別の診断精度については多数の報告がある[13)]。

症例提示

●症例1：浸潤性乳管癌（図4）

65歳，女性。約18mm大の辺縁分葉状を呈する腫瘤が認められる。この腫瘤は，DWIにて辺縁を中心に高信号を呈する。lobulated shape/irregular-spiculated marginを呈し，ダイナミックスタディでは，辺縁はrapid-washout patternである。中心部はpersistent patternで線維化が推察される。術後病理では，13mm×11mmの浸潤性乳管癌（硬癌）と診断された。中心部は間質増生が強く，辺縁部は腫瘍細胞が孤在性に索状に配列し，脂肪織まで浸潤していた。

●症例2：非浸潤性乳管癌が大部分を占める浸潤性乳管癌（図5）

47歳，女性。約20mmの嚢胞内に乳頭状に発育する充実部が認められ（⇒），これより連続して乳頭側方向に病変が進展している（▷）。腫瘍はDWIにて高信号を呈する。clustered ring enhancementがbranching-ductalの形態をとり，segmentalに分布する。ダイナミックスタディではrapid-washout patternである。術後病理では，非浸潤癌が大部分を占める浸潤性乳管癌と診断された。13mm×8mmの嚢胞内に異型腺管の乳頭状増殖が見られ，一部で壁内に2mm×2mmの範囲で微小浸潤を認めた。また，嚢胞より乳頭側に，papillary type主体の乳管内病変が約30mmにわたり認められた。

●症例3：粘液癌（図6）

33歳，女性。約30mmの境界明瞭な腫瘤が認められる。STIRにて高信号を呈する。DWIでは拡散の低下は比較的

症例—2　　非浸潤性乳管癌が大部分を占める浸潤性乳管癌（図5）

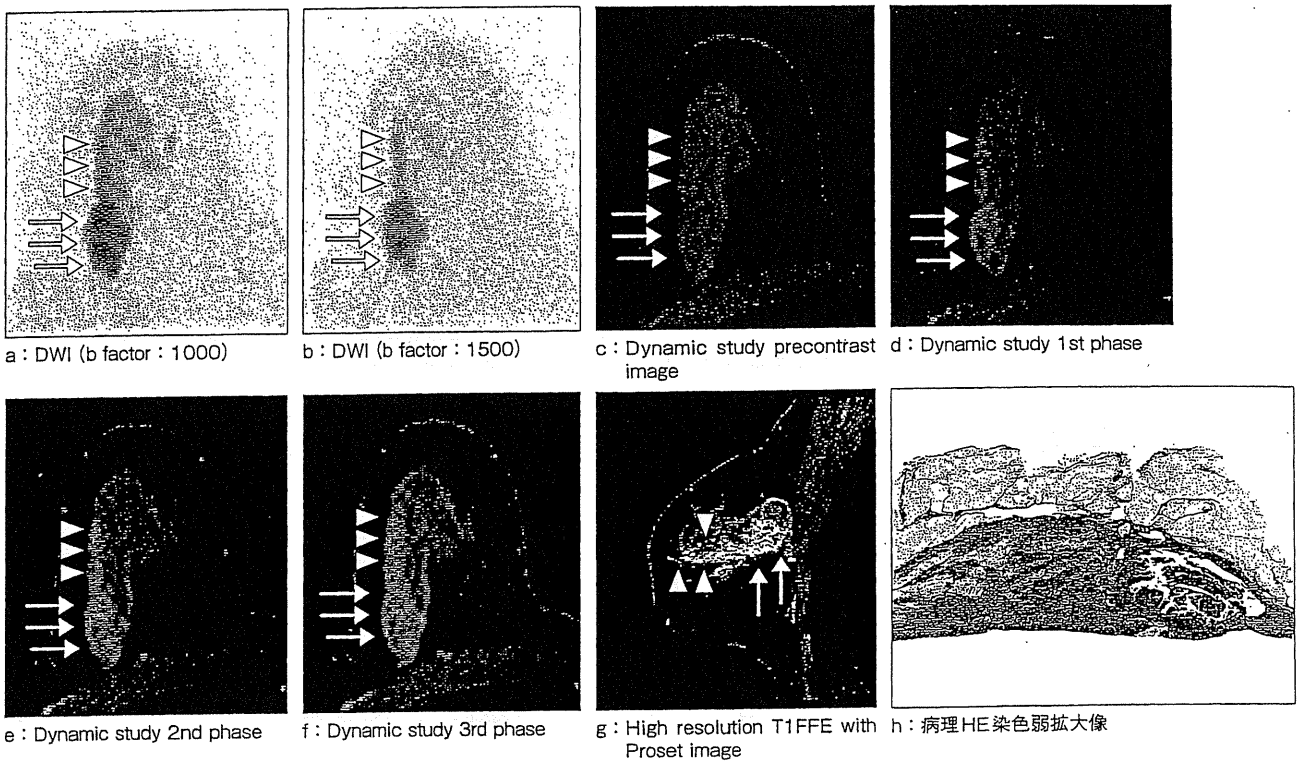

a：DWI（b factor：1000）　b：DWI（b factor：1500）　c：Dynamic study precontrast image　d：Dynamic study 1st phase

e：Dynamic study 2nd phase　f：Dynamic study 3rd phase　g：High resolution T1FFE with Proset image　h：病理HE染色弱拡大像

図5　症例2：非浸潤性乳管癌が大部分を占める浸潤性乳管癌（47歳，女性）

症例—3　　粘液癌（図6）

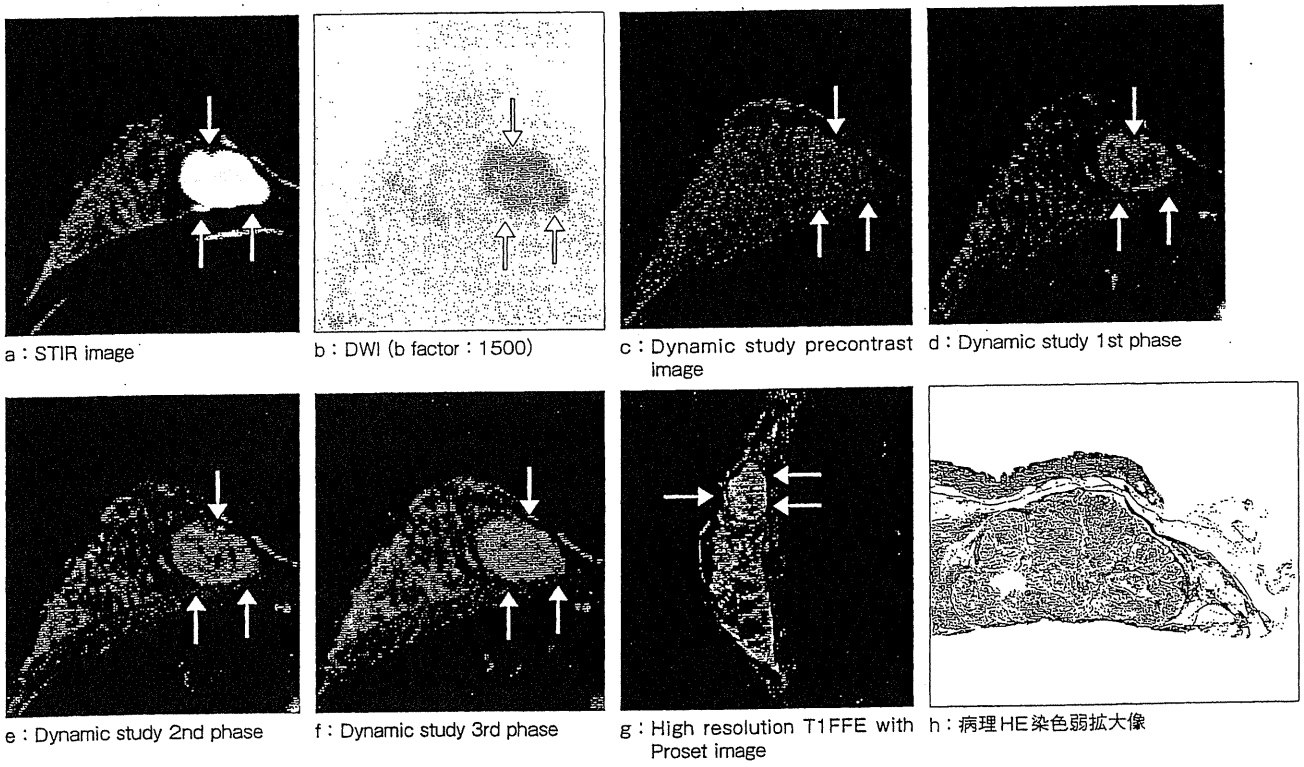

a：STIR image　b：DWI（b factor：1500）　c：Dynamic study precontrast image　d：Dynamic study 1st phase

e：Dynamic study 2nd phase　f：Dynamic study 3rd phase　g：High resolution T1FFE with Proset image　h：病理HE染色弱拡大像

図6　症例3：粘液癌（33歳，女性）

症例—4　乳管内乳頭腫（図7）

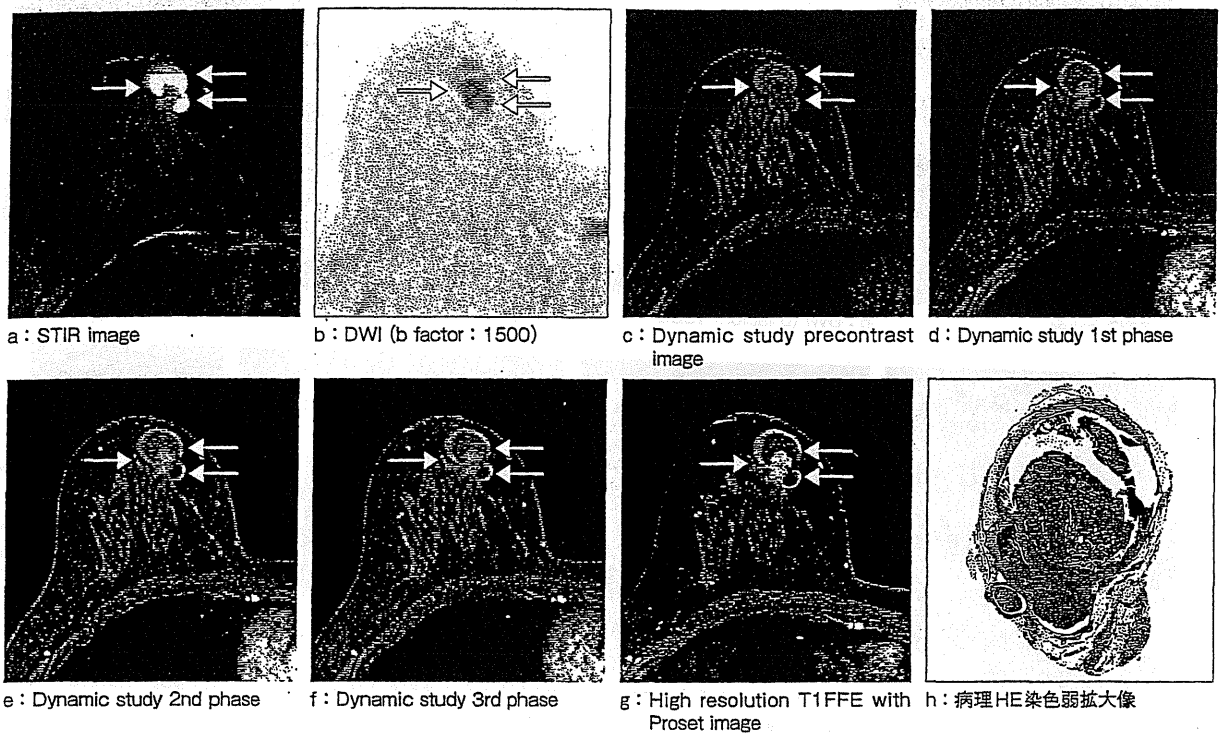

図7　症例4：乳管内乳頭腫（48歳，女性）

少ない。lobulated shape/smooth marginを呈し，ダイナミックスタディではrapid-persistent patternである。術後病理では，30mm×20mm大の圧排性に周囲脂肪織まで浸潤する粘液癌と診断された。豊富な粘液中にがん細胞（島）が比較的高密度に認められた。

●症例4：乳管内乳頭腫（図7）

48歳，女性。嚢胞内に乳頭状に発育する充実部が認められる。充実部はDWIにて高信号を呈する。積極的に嚢胞外へ進展している所見は認められない。充実部はダイナミックスタディにてrapid-washout patternを呈する。術後病理では，嚢胞内に線維性血管間質を有し，乳頭状に増殖する腫瘍を認めた。二相性が保持されていることから乳管内乳頭腫と診断された。明らかな嚢胞外への浸潤は認められなかった。

●症例5：線維腺腫と乳管乳頭腫症（図8）

64歳，女性。約10mmの結節（↓）と約5mmの結節が2個（△）認められる。いずれも境界明瞭・平滑で，10mm大の結節はDWIで低～等信号，5mm大の結節は高信号を呈する。いずれもSTIRにて等信号を呈し，内部構造は明らかではない。round-oval shape/smooth marginを呈し，ダイナミックスタディでは，10mm大の結節がmedium-persistent pattern，5mm大の結節がrapid-washout patternである。術後病理では，10mm大の結節は一部に器質化を伴った管内型線維腺腫（↓），5mm大の結節は乳管上皮増生を高度に伴った乳管乳頭腫症（△）と診断された。

◎

乳腺造影MRIについて，ダイナミックスタディを中心に撮像法と症例を提示し概説した。乳腺MRIはダイナミックスタディが中心となるが，一方で，報告にもあるように，血流情報に形態情報を加えることで診断能は向上する[11),12)]。また，最近ではDWIやMRSの臨床応用も盛んであり[13),14)]，これらの画像も加味して総合的に診断することが肝要である。

症例—5　線維腺腫と乳管乳頭腫症（図8）

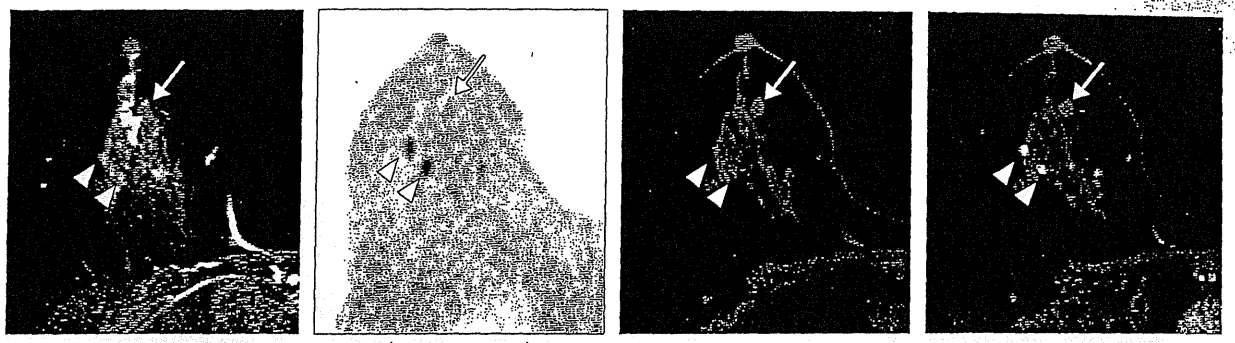

a：STIR image　b：DWI (b factor：1500)　c：Dynamic study precontrast image　d：Dynamic study 1st phase

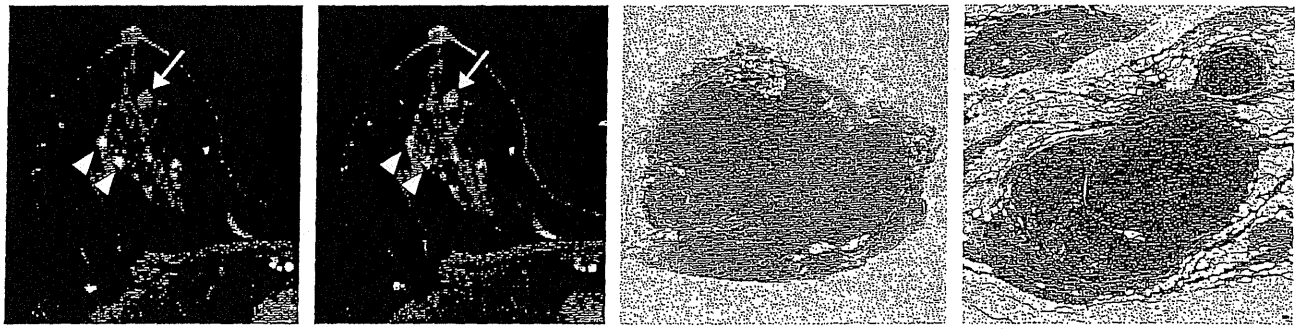

e：Dynamic study 2nd phase　f：Dynamic study 3rd phase　g：病理HE染色弱拡大像（線維腺腫）　h：病理HE染色弱拡大像（乳管乳頭腺症）

図8　症例5：同一症例に発生した線維腺腫（⇩）と乳管乳頭腫症（△）（64歳，女性）

●参考文献

1) Breast imaging reporting and data system ; BI-RADS (Reston, V.A., ed), 4th ed., American College of Radiology, 2003.
2) Heywang, S.H., Hahn, D., Schmidt, H., et al. : MR imaging of the breast using gadolinium-DTPA. *J. Comput. Assist. Tomogr.*, **10**, 199～204, 1986.
3) Kaiser, W.A., Zeitler, E. : MR imaging of the breast ; Fast imaging sequences with and without Gd-DTPA ; Preliminary observations. *Radiology*, **170**, 681～686, 1989.
4) Boetes, C., Barentsz, J.O., Mus, R.D., et al. : MR characterization of suspicious breast kesions with a gadlinium-enhanced Turbo FLASH subtraction technique. *Radiology*, **193**, 777～781, 1994.
5) Gilles, R., Guinebretiere, J.M., Lucidarme, O., et al. : Nonpalpable breast tumors ; Diagnosis with contast-enhanced subtraction dynamic MR imaging. *Radiology*, **191**, 625～631, 1994.
6) Kuhl, C.K., Mielcareck, P., Klaschik, S. et al. : Dynamic breast imaging ; Are signal intensity time course data useful for differential diagnosis of enhancing lesions?. *Radiology*, **211**, 101～110, 1999.
7) Pierce, W.B., Harms, S.E., Flamig, D.P., et al. : Three-dimensional gadolinium-enhanced MR imaging of the breast ; Pulse sequence with fat suppression and magnetization transfer contrast. *Radiology*, **181**, 757～763, 1991.
8) Harms, S.E., Flamig, D.P., Hesley, K.L., et al. : MR imaging of the breast with rotating delivery of excitation off resonance ; Clinical experience with pathologic correlation. *Radiology*, **187**, 493～501, 1993.
9) Fischer, U., Kopka, L., Grabbe, E. : Breast carcinoma ; Effect of preoperative contrast-enhanced MR imaging on the therapeutic approach. *Radiology*, **213**, 881～888, 1999.
10) MARIBS study group : Evaluation of a prospective scoring system designed for a multicenter breast MR imaging screening study. *Radiology*, **239**, 677～685, 2006.
11) Tozaki, M., Igarashi, T., Fukuda, K. : Positive and negative predictive value of BI-RADS-MRI descriptors for focal breast masses. *Magn. Reson. Med. Sci.*, **5**, 7～15, 2006.
12) Kinkel, K., Helbich, T.H., Esserman, L.J., et al. : Dynamic high-spatial-resolution MR imaging of suspicious breast lesions ; Diagnostic criteria and interobserver variability. *Am. J. Roentgenol.*, **175**, 35～43, 2000.
13) Kuroki, Y., Nasu, K., Kuroki, S., et al. : Diffusion-weighted imaging of breast cancer with the sensitivity encoding technique ; Analysis of apparent diffusion coefficient value. *Magnet. Res. Med. Sci.*, **3**, 79～85, 2004.
14) Tozaki, M., Sakamoto, M., Oyama, Y., et al. : Monitoring of early response to neoadjuvant chemotherapy in breast cancer with H MR Spectroscopy ; Comparison to sequential 2-[18F]-fluorodeoxyglucose positron emission Tomography. *J. Magn. Reson. Imaging*, **28**, 420～427, 2008.

日本医師会雑誌　第138巻・特別号（1）　平成21（2009）年6月15日発行　昭和23年4月24日第3種郵便物認可

日本医師会雑誌　第138巻・特別号（1）

生涯教育シリーズ――76

THE JOURNAL OF THE JAPAN MEDICAL ASSOCIATION

がん診療update

監　修　跡見　裕

編　集　島田安博
杉原健一
谷本光音
森　正樹
吉村泰典

編集協力　阿部展次

JMA 日本医師会

消化管造影検査

Alimentary Tract Imaging by Barium Studies

関口隆三　石川　勉
Ryuzo Sekiguchi　Tsutomu Ishikawa

はじめに

消化管造影検査は得られた画像が客観的で，検査自体による侵襲性が少ないことから，内視鏡検査が普及しつつある今なお，集団検診を含め広く行われている．本稿では消化管造影検査の利点，特にがん診療における有用性について，また内視鏡検査とのかかわり方について述べる．

消化管造影検査の利点

消化管造影検査が優れているのは得られた画像の客観性であり，病変の位置や範囲，周囲臓器との関係，また消化管壁の伸展性や変形所見などを直感的に把握できる概観撮影法としての有用性が非常に高い点である．内視鏡検査では，病変が視野全体に拡がっているようなびまん性疾患（図1）や，視野に入りきらない大きな病変では，病変の全体像（病変そのもの，および病変の消化管の中での占拠部位など）の把握が困難な場合がしばしば経験される．横行結腸や過長S状結腸においては，病変の存在位置を見誤ることもあり，総腸間膜症などの解剖学的・先天的走行異常症例は，消化管造影検査でないと把握することが困難であることが多い．

消化管造影検査は十二指腸憩室や大腸憩室の診断にも有効で，憩室周囲炎および膿瘍形成を合併し，管腔の狭窄をきたしているような場合においては病態を正確に把握・診断することが可能である．腹膜播種や腫瘍浸潤に伴う消化管狭窄にも造影検査は有効で，病変が多発している場合や消化管の狭窄の強い場合には特に有用である．腫瘍や出血，微細血管異常などの小腸病変の検出には，近年小腸内視鏡検査（ダブルバルーン法）が普及しつつあるが，経口小腸造影検査は簡便で侵襲も少なく，現在でも有用な検査法である（図2）．

がん診療においては，病変の質的診断を行ううえで，また病変の拡がりおよび深達度診断，切除線の決定などの外科的治療を行ううえで，客観的な画像（情報）を提供する消化管造影検査は治療前検査として欠くことができない検査法に位置づけられている．また消化管造影検査は治療経過や経過観察における経時的（遡及的）形態変化の客観的な把握にも有用である．図3に胃がんにおける病変と食道胃接合部との距離，図4に直腸がんにおける病変とHerrmann線との距離を描出したX線像を示す．

内視鏡検査との関係

内視鏡検査は機動性に富み，生検による病理診断や止血，ポリペクトミーなどの治療が行える利点を有していることから急速に普及しつつある．内視鏡検査で色調の変化として捉えられるような形態的には変化に乏しい病変は，バリウムと空気により病変を描出させる消化管造影検査では所見を拾いきれず，見逃されてしまうこともある．消化管診断においては，消化管造影検査，内視鏡検査それぞれの特長を生かしての検査の組み合わせ（両者の併用）が消化管疾患，とりわけがん診療の診断効率の向上につながっている．

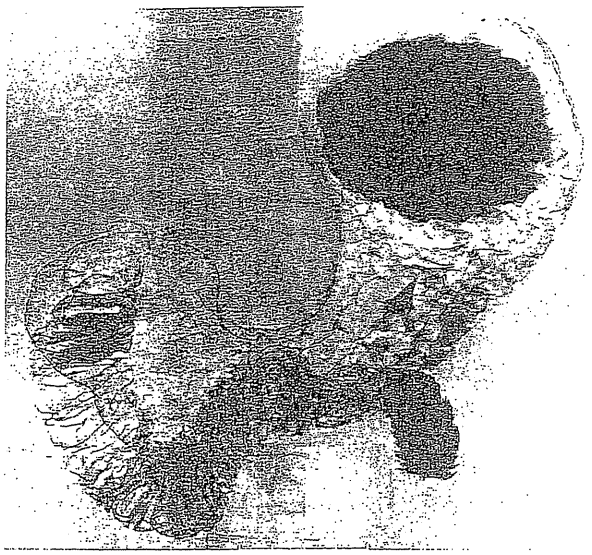

図1　概観観察法としての消化管造影検査の有用性
穹窿部より前庭部にまたがる広範囲にわたる著明な胃壁の伸展不良がみられる．体下部小彎には潰瘍面がみられ，type 3 スキルス胃がんと診断される．

図2　経口小腸造影検査による小腸腫瘍の描出
右腸骨稜レベルの小腸（空腸）に，約2～3cmにわたり全周性狭窄（apple core sign）を認める（矢印）．

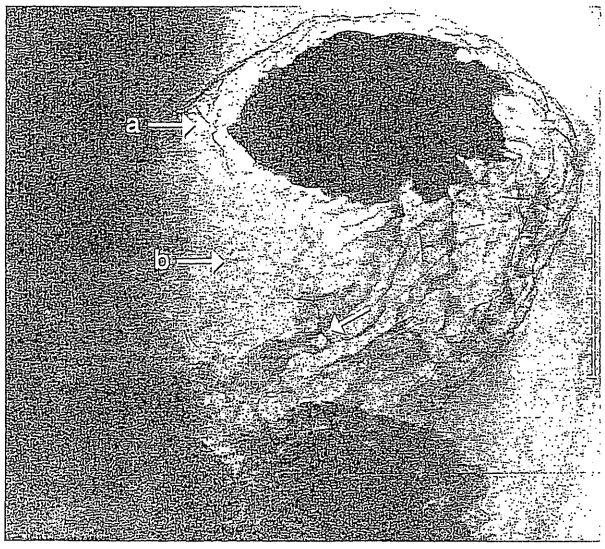

図3　病変と食道胃接合部との距離の描出
体中部後壁のtype 3 病変（矢印）．食道胃接合部（a）までの距離は約5cm．病変の口側に生検による小さなバリウム斑（b）がみられる．

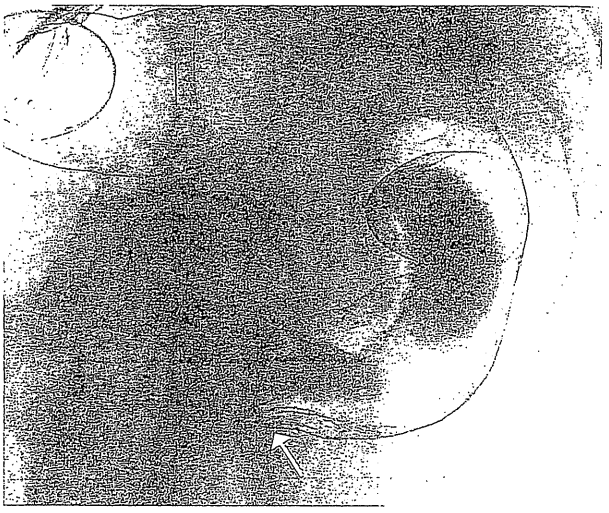

図4　病変とHerrmann線との距離の描出
直腸Rb前壁を中心とするtype 2病変．大きさは約5cm．側面変形を認め，深達度はMP以深と判断される．Herrmann線（矢印）までの距離は約4cm．

特集
膵・胆道癌遠隔転移診断：2009
胆と膵 Vol. 30 (9) p. 945～950, 2009

造影超音波による肝転移診断*

関口 隆三[1)]・山邉裕一郎[1)]・平原 美孝[1)]・黒木 嘉典[1)]・山本 孝信[1)]
吉田 慶之[1)]・小林 望[1)]・吉竹 直人[1)]・斎藤奈津子[1)]

要約：悪性疾患における肝転移巣の存在診断は治療方針決定に際し重要であり，画像診断が進歩した今日なお十分とは言い切れない。全世界に先駆けてわが国で臨床応用が可能となった超音波造影剤 Sonazoid® は micro bubble を非破壊で映像化するため，肝臓の造影効果の持続性が高く，また繰り返し検査・検索できることから，肝実質相における腫瘍描出能に非常に優れている。肝臓の観察が十分できる術者であれば Gd-EOB MRI と同等またはそれ以上の肝腫瘍検出能が期待できる。当院では造影超音波検査を肝転移巣検索における精査として行っており，とりわけ膵癌病期診断における意義は高い。造影超音波検査は明瞭で持続性の Vascular imaging もリアルタイムに提供できることから，悪性疾患の治療方針決定（病期診断）や化学療法などの治療効果判定などの機能評価の指標としての応用も期待される。

Key words：Sonazoid，超音波造影剤，肝腫瘍，転移

はじめに

2007年1月より全世界に先駆けてわが国で発売された次世代超音波造影剤 Sonazoid®の登場は，肝臓の超音波診断・治療の精度向上に拍車をかけることは間違いなく，超音波を取り巻く画像診断環境は今，大きく変わりつつある。安定した肝実質相（Post vascular phase）の提供は肝腫瘍検出能の向上をもたらし（図1），持続性の vascular imaging は腫瘍内血流の検討，すなわち腫瘍の viability の有無の判定を可能としている[1,2]（図2）。

本稿では，転移性肝腫瘍診断における Sonazoid®造影超音波検査の特徴や有用性，将来展望などについて述べる。

Ⅰ．Sonazoid® 造影超音波検査の特徴

これまでの超音波造影剤 Levovist®が，micro bubble を破壊・映像化していたのに対し，Sonazoid®は低～中音圧では micro bubble を非破壊で映像化することができるため，持続した造影効果を観察することが可能となった。Levovist®の micro bubble は超音波照射により容易に破壊され，一瞬にして超音波照射部の micro bubble は消失する。したがって Levovist®を用いた場合は，一般に間欠送信下（非連続的）に造影効果の観察を行わなければならず，肝実質相の観察は1回のスイープスキャンのみに限られるなどの大きな制限があった。Sonazoid®は低～中音圧では micro bubble を破壊することなく連続送信にて繰り返し肝内をくま無く観察することができ，また肝臓の Kupffer 細胞内に取り込まれることから，癌の肝転移巣検索（病期診断）の詳細な検討が可能となった。また肝腫瘍内血流の連続観察がリアルタイムに可能なことから（図3），肝の質的診断，転移性肝腫瘍の治療支援および治療効果判定の精度向上に大いに貢献するものと期待されている[1,2]。

Ⅱ．転移性肝腫瘍の診断手順

当院では，Sonazoid®造影超音波検査（以下造影超音波検査）は肝転移巣の精査―肝転移巣検索および治

* Hepatic Metastases：Diagnosis with Sonazoid-enhanced Sonography

1) 栃木県立がんセンター画像診断部（〒320-0834 宇都宮市陽南 4-9-13）

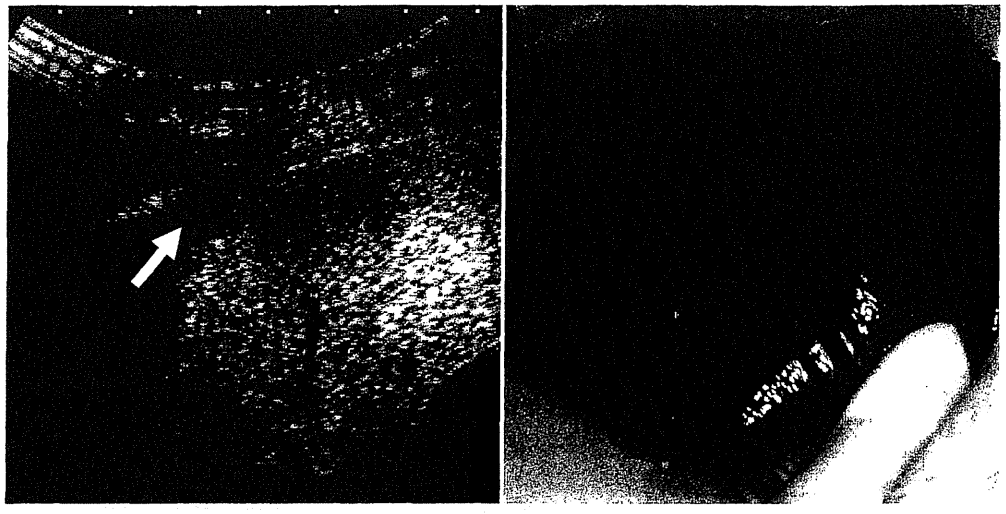

a|b

図 1　肝転移巣の検出
60 歳女性，膵頭部癌肝転移。造影超音波検査（Post vascular phase）では S8 肝表にφ4 mm の内部血流を伴う SOL（→）を認め転移と診断（a）。開腹時，転移巣を確認（b，→）。

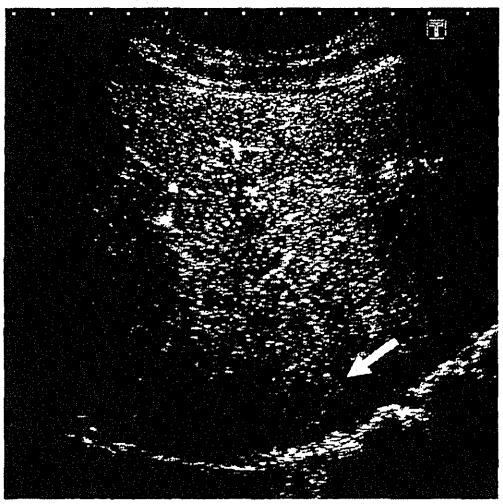

図 2　Vascular imaging
68 歳男性，胃癌肝転移。肝 S7，26×20×20 mm 大の等エコー腫瘤は早期濃染し（Early vascular phase，→），すぐに wash-out を認め，転移と診断。

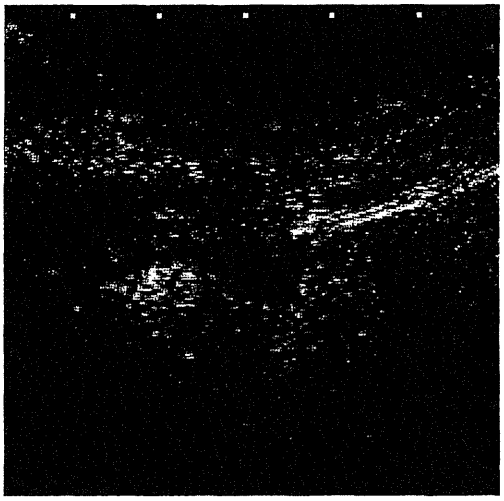

図 3　腫瘍内血流の観察
67 歳男性。膵体尾部癌肝転移。肝表にみられるφ8 mm の SOL 内を流れる micro bubble（低エコー腫瘤内の高エコースポット）が明瞭に観察される。

療効果判定一目的に施行している。図 4 に当院における転移性肝腫瘍診断のフローチャートを示す。経過観察の場合，原発巣や病期，CEA や CA19-9 などの腫瘍マーカー値の変動の有無により検査の施行間隔は異なってくるが，一般に通常の超音波検査（以下単純超音波検査）は年 2（～4）回，造影 CT 検査は年 1（～2)回程度としている。精査が必要と判断された場合は造影超音波検査と 2008 年 4 月からは EOB・Primovist を用いた Gd-EOB MRI を並行して行っている。また，手術適応の決定にあたっては血管造影下 CT（CTA，CTAP）を施行し，それぞれの画像所見をあわせ総合的に最終診断を下している。

Ⅲ．検査装置・手技

当院で造影超音波検査に用いている超音波診断装置は Aplio XG（東芝メディカルシステムズ）および Logiq7（GE 横河メディカルシステム）である。探触子はコンベックス型のものを用い，肝右葉横隔膜下の観察が肋間よりしにくい場合は視野角の広いマイクロコンベックス型のものを適宜用いている。

造影超音波検査は単純超音波検査に引き続き施行している。前腕に留置した 22 G の留置針より自動注入器 Medrad Pulser®（日本メドラッド）を用い，0.00375～